Journal of
Medicinal Chemistry
Article

Synthesis, in Vitro and in Vivo Biological Evaluation, Docking Studies, and Structure−Activity Relationship (SAR) Discussion of Dipeptidyl Boronic Acid Proteasome Inhibitors Composed of β-Amino Acids

Yongqiang Zhu,*,[†] Xinrong Zhu,[†] Gang Wu,[†] Yuheng Ma,[†] Yuejie Li,[†] Xin Zhao,[†] Yunxia Yuan,[†] Jie Yang,[†] Sen Yu,[†] Feng Shao,[†] Runtao Li,[‡] Yanrong Ke,[‡] Aijun Lu,[†] Zhenming Liu,[‡] and Liangren Zhang[‡]

[†]*Jiangsu Simcere Pharmaceutical Research Institute and Jiangsu Key Laboratory of Molecular Targeted Antitumor Drug Research, No. 699-18 Xuan Wu Avenue, Xuan Wu District, Nanjing 210042, PRC, and* [‡]*State Key Laboratory of Natural and Biomimetic Drugs, School of Pharmaceutical Sciences, Peking University, No. 38 Xueyuan Road, Haidian District, Beijing 100191, PRC*

A series of novel dipeptidyl boronic acid proteasome inhibitors composed of β-amino acids were synthesized, in vitro and in vivo biologically evaluated, and theoretically modeled for the first time. From the screened racemic compounds in enzyme, **4i** was the most active. The IC_{50} value of its pure enantiomer **4q** was 9.6 nM, 36-fold more active than its isomer **4p** and as active as the marketed bortezomib in inhibiting human 20S proteasome. This candidate also showed good activities with IC_{50} values nearly less than 5 μM against several human solid and hematologic tumor cell lines. Safety evaluation in vivo with zebrafish and Sprague−Dawley (SD) rats showed that the candidate **4q** was less toxic than bortezomib. Pharmacokinetic profiles suggested candidate **4q** showed a more plasma exposure and longer half-life than bortezomib. Docking results indicated that **4q** nearly interacted with 20S proteasome in a similar way as bortezomib.

Introduction

The ubiquitin−proteasome pathway (UPP[a]) is responsible for the degradation of more than 80% normal and abnormal intracellular proteins.[1] It has been shown that this pathway is central to normal cellular homeostasis including cell cycle regulation, DNA repair, sodium channel function, regulation of immune and inflammatory responses, and cellular response to stress.[2−4] A growing body of evidence suggested that derangements of UPP could lead to many disorders, such as malignancies, neurodegenerative diseases, and possible systematic autoimmunity.[5] At the heart of this system is the 26S proteasome, which is a dynamic multisubunit proteolytic complex with a molecular weight of 700 kDa and functions in eukaryote as a key enzyme for nonlysosomal degradation.[6] The cylindered 26S proteasome is composed of two subcomplexes: one multicatalytic proteinase complex (MPC) 20S proteasome and two regulatory particles 19S proteasome (RP). The 20S proteasome is the proteolytic site and shows three different types of catalytic activities, chymotrypsin-like (CT-L, β5 subunit), trypsin-like (T-L, β2 subunit), and cas-
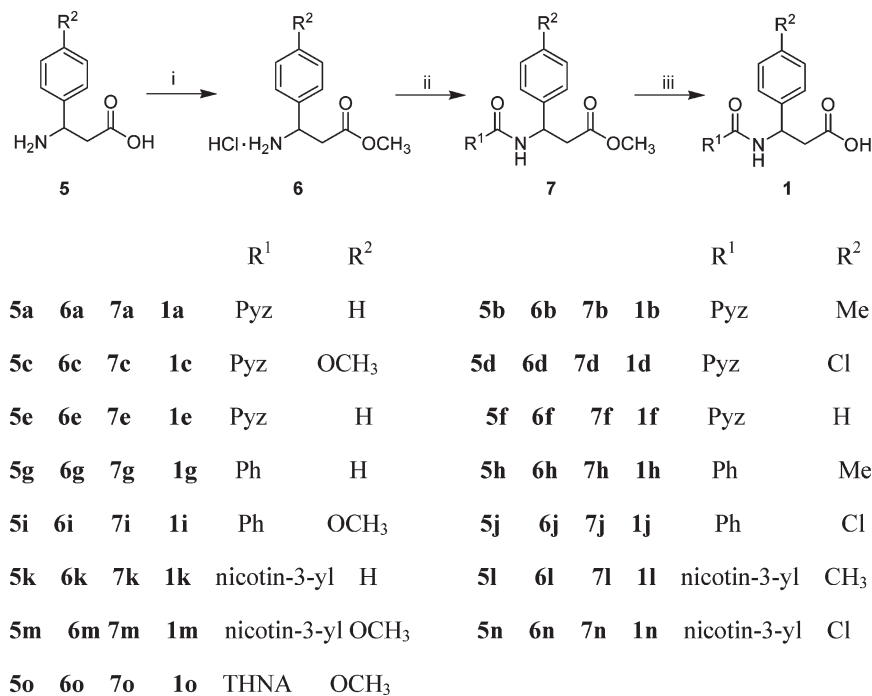
pase-like (PGPH, β1 subunit). The 19S RP caps at both ends of the CP and controls the recognition of the ubiquinated proteins before they enter the 20S proteasome and therein are degraded into pieces of small amino acids.

The realization that the proteasome is so critically related to the development of a number of major human diseases promoted research into the design and synthesis of various proeasome inhibitors and the evaluation of their therapeutic potentials. In recent years, there has been a great deal of interest in proteasome inhibitors as a novel class of anticancer candidates and some of them entered clinical trial, such as bortezomib and salinosporamide A (also named NPI-0052).[7−9] The dipeptidyl boronic acid bortezomib was approved to be used for the treatment of relapsed and refractory multiple myeloma (MM) in 2003 and mantle cell lymphoma (MCL) in 2006. Though bortezomib therapy has proven to be successful for the treatment of hematologic tumor and potentially good for other types of cancer,[10,11] prolonged treatment is associated with toxicity and development of drug resistance.[12]

On the basis of our accumulated knowledge of the structure of proteasome and its inhibitors,[13−15] we recently disclosed a comprehensive understanding of dipeptidyl boronate proteasome inhibitors composed of α-amino acids.[16] In an effort to design the second generation proteasome inhibitors as anticancer agents with less toxicity, nowadays by use of scaffold migration method, we directed our work to the exploration of dipeptidyl boronic acids containing β-amino acids. In several cases, the substitution of an α-amino acid for their β-isomer in biologically active peptides resulted in an increased activity and enzymatic stability.[17,18] β-Peptides, formed by β-amino acids having an extra backbone carbon, have been intensely

---

*To whom correspondence should be addressed. Phone: 86-25-85566666-1726. Fax: 86-25-85566666-1835. E-mail: zhyqscu@hotmail.com.

[a] Abbreviations: SAR, structure−activity relationship; UPP, ubiquitin−proteasome pathway; MM, multiple myeloma; MCL, mantle cell lymphoma; MPC, multicatalytic proteinase complex; RP, regulatory particle; CT-L, chymotrypsin-like activity; T-L, trypsin-like activity; PGPH, postglutamyl peptide hydrolysis activity; IC_{50}, inhibition constant; DCC, *N,N*'-dicyclohexylcarbodiimide; HOBt, 1-hydroxybenzotriazole; EDC, 1-ethyl-3-(3-dimethylaminopropyl)carbodiimide; DIPEA, *N,N*-diisopropylethylamine; sd, standard deviation; SD, Sprague−Dawley; rmsd, root-mean-square deviation; LLOD, lower limit of detection; SRM, selected reaction monitoring.

Scheme 1. General Synthesis of Racemized N-Terminal Protected β-Amino Acids **1a–o**[a]

				R[1]	R[2]					R[1]	R[2]
5a	**6a**	**7a**	**1a**	Pyz	H	**5b**	**6b**	**7b**	**1b**	Pyz	Me
5c	**6c**	**7c**	**1c**	Pyz	OCH₃	**5d**	**6d**	**7d**	**1d**	Pyz	Cl
5e	**6e**	**7e**	**1e**	Pyz	H	**5f**	**6f**	**7f**	**1f**	Pyz	H
5g	**6g**	**7g**	**1g**	Ph	H	**5h**	**6h**	**7h**	**1h**	Ph	Me
5i	**6i**	**7i**	**1i**	Ph	OCH₃	**5j**	**6j**	**7j**	**1j**	Ph	Cl
5k	**6k**	**7k**	**1k**	nicotin-3-yl	H	**5l**	**6l**	**7l**	**1l**	nicotin-3-yl	CH₃
5m	**6m**	**7m**	**1m**	nicotin-3-yl	OCH₃	**5n**	**6n**	**7n**	**1n**	nicotin-3-yl	Cl
5o	**6o**	**7o**	**1o**	THNA	OCH₃						

[a] Reagents and conditions: (i) CH_3OH, $SOCl_2$, 0 °C to room temp; (ii) R^1COOH, DCC, HOBt, NMM, THF, 0 °C; (iii) (1) 2 N NaOH, acetone/H_2O, 0 °C; (2) 2 N HCl, 0 °C.

studied for years to discover stable well-ordered secondary structures.[19–22] Furthermore, the use of β-amino acids as the building block of proteasome inhibitors has never been reported.

Nowadays, because of the low cost of zebrafish and its high degree of similarity with humans in the drug responses,[23,24] drug-screening assays using zebrafish are increasingly becoming popular.[25,26] Such inexpensive and convenient animal models have been applied in a variety of assays for assessing cardiotoxicity,[27] hepatotoxicity,[28] neurotoxicity,[29] and mutagenesis.[30]

In this manuscript, we described the synthesis, biological evaluation, SAR investigation, and toxicity assessment with zebrafish and SD rats, pharmacokinetic profiles, and docking studies for a series of dipeptidyl boronic acids composed of β-amino acids as the novel proteasome inhibitors. Enzymatic and cellular activity profiles of the most active racemate (±)-**4i** were compared to those of its pure enantiomers **4p** and **4q**. The in vivo safety profiles of the two isomers and bortezomib were evaluated and compared. Binding modes of isomers **4p** and **4q** with 20S proteasome were studied in detail with the docking method.

Results and Discussion

Chemistry. The preparation of racemized β-amino acids **1** was illustrated in Scheme 1. β-Amino acids **5** were purchased from commercial sources. Methyl ester hydrochlorides **6** were synthesized by the traditional $MeOH/SOCl_2$ method. After coupling of acid R^1COOH with **6** using the traditional liquid peptide synthesis procedures,[31] N-terminal protected methyl esters **7** were obtained, which were saponificated and acidified to give acids **1** in high yield.

Chiral β-amino acids **1p** and **1q** were prepared according to Scheme 2 by applying a reported procedure.[32,33] The commercially available 4-methoxybenzaldehyde was treated

with n-BuLi and *tert*-butyl diethylphosphonoacetate **8** at −78 °C, giving *tert*-butyl α,β-unsaturated esters **9**, which was purified by chromatography on silica gel and obtained in high yield.

The conjugate additions were carried out between esters **9** and the homochiral (R)- and (S)-N-benzyl-N-(α-methylbenzyl)amides **10a** and **10b**, respectively, in the presence of n-BuLi at −78 °C to produce the (R)- and (S)-enantiomers of the β-amino acid esters **11a** and **11b** in high yields. The N-debenzylation products **12a** and **12b** were obtained from their corresponding N-protected esters **11a** and **11b** in a methanol−acetic acid−water mixture system catalyzed by $Pd(OH)_2$ on C in hydrogen atmosphere. After filtration to remove the heterogeneous catalyst and concentration of the resulting reaction mixture, the crude products **12a** and **12b** were purified by chromatography in the presence of triethylamine and obtained in moderate to high yield.

Coupling reactions were performed between benzoic acid and β-amino esters **12a** and **12b** in the presence of DCC/HOBt coupling reagent to prepare N-terminal protected *tert*-butyl ester β-amino acids, which were hydrolyzed by HCl/Et_2O to remove the ester, giving N-terminal protected β-amino acids **1p** and **1q** in moderate yields after crystallization. Chiral HPLC indicated that no isomers were detected for both compounds.

The generalized preparation of dipeptidyl boronic acids **4** is illustrated in Scheme 3. The key boronate intermediates, hydrochloride salt of aminoboronates **2**, were prepared in moderate to high yields following our reported method.[16] Finally, coupling of aminoboronates **2** with various acids **1** in the presence of 1-ethyl-3-(3-dimethylaminopropyl)carbodiimide hydrochloride (EDC·HCl) and HOBt afforded the dipeptidyl boronates **3** which were not purified and directly transesterificated with isobutylboronic acid under acid conditions to give boronic acids **4**.

Scheme 2. General Synthesis of Chiral N-Terminal Protected β-Amino Acids **1p** and **1q**[a]
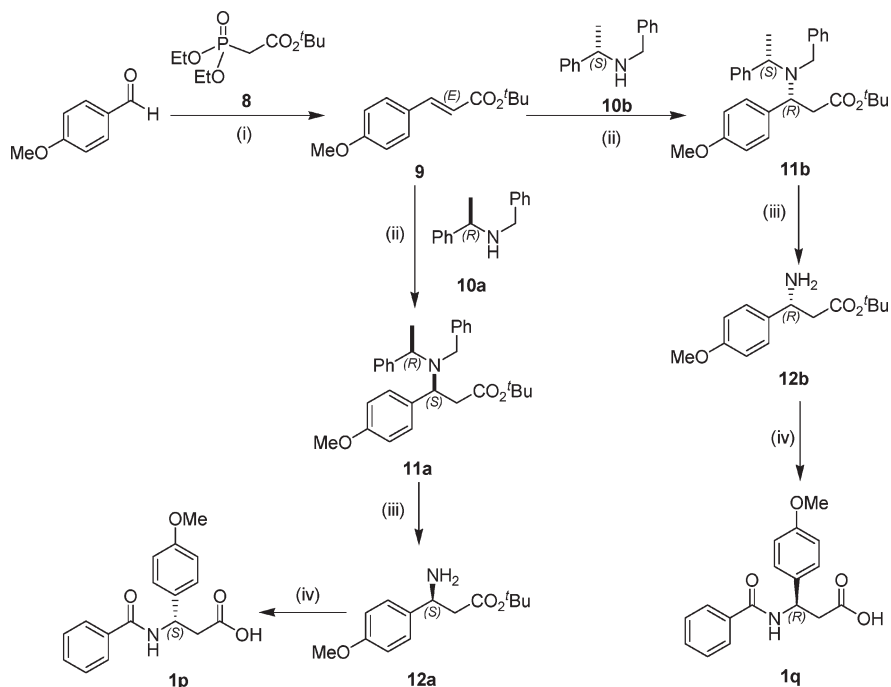
[a] Reagents and conditions: (i) (EtO)$_2$POCH$_2$CO$_2$^{t}Bu, *n*-BuLi, THF, −78 °C to room temp, 86%; (ii) **10a** or **10b**, *n*-BuLi, THF, −78 °C, 4 h, 85% for **11a**, 88.4% for **11b**; (iii) H$_2$, Pd(OH)$_2$/C, MeOH, H$_2$O, AcOH, room temp, 24 h, 73.4% for **12a**, 89.2% for **12b**; (iv) (1) PhCOOH, DCC, HOBt, NMM, THF, 0 °C; (2) HCl/Et$_2$O, 0 °C, 18 h, 58.6% for **1p**, 61.6% for **1q**.

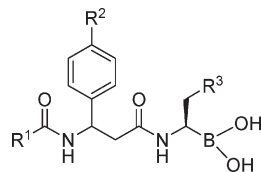**Scheme 3.** General Synthesis of Dipeptidyl Boronic Acids **4**[a]
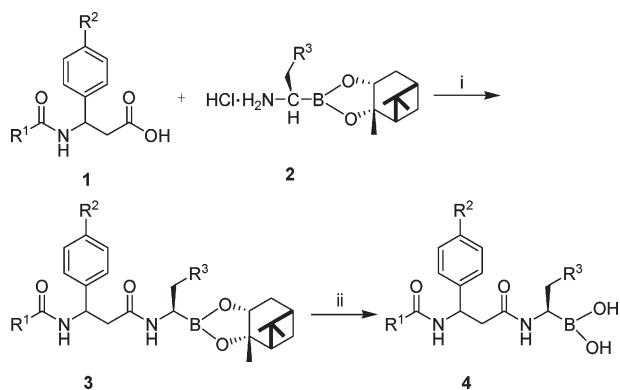
[a] Reagents and conditions: (i) EDC·HCl, HOBt, DIPEA, CH$_2$Cl$_2$, −15 °C to room temp; (ii) isobutylboronic acid, 2 N HCl, MeOH, hexane.
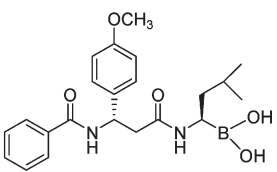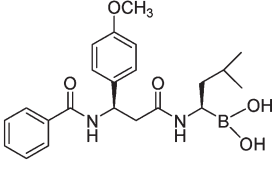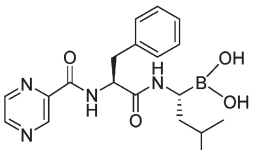
Biology. Enzyme. Because of the fact that no SAR of such novel compounds has been reported, different substituents of three positions R^1, R^2, and R^3 were initially designed according to the following rules: for R^1 substituents, aromatic rings with or without N atoms were employed; for R^2 substituents, electron-withdrawing or electron-donating groups were used; for R^3 substituents, aliphalic or aromatic groups were considered. And the potency of final compounds was evaluated in the human 20S chymotrypsin-like activity. Table 1 summarized the structures and inhibition activities of the designed dipeptidyl boronic acids. Because of the more complex and difficult synthesis of chiral β-amino acid compared with its racemate, for SAR discussion in this work, (±) β-amino acids at R^2 position were employed for fast biological screening. Table 1 showed that all the compounds inhibited the chymotrypsin-like activity of 20S pro-

teasome with IC$_{50}$ values widely ranging from 9.6 to 664 nM, indicating that internal SAR existed. Especially the pure enantiomer **4q** was found to be highly potent with an IC$_{50}$ of 9.6 nM, which was being regarded as an anticancer drug candidate to be developed.

Pyrazin-2-yl group was a component of the marketed bortezomib, so this fragment was also used in the initial design in R^1 position. Exploration of substituents at R^1 position revealed the following activity order: phenyl (**4i**, 12.5 nM) > nicotin-3-yl (**4m**, 35 nM) > pyrazin-2-yl (**4c**, 134 nM) > 5,6,7,8-tetrahydronaphalen-1-yl (**4o**, 161 nM), groups at R^2 and R^3 positions of which were substituted by 4-methoxy and isopropyl groups, respectively. Different aromaticity of these four substituents may account for the different activities. β-Amino acid scanning of the R^2 position, including hydrogen, methyl, methoxy, and chloro substituted β-phenylalanines, demonstrated that electron-donating groups (such as methyl and methoxy substituted **4h** and **4i**) were more beneficial to activities than electron-withdrawing ones (such as chloro substituted **4j**), and the same conclusion was also drawn by the comparison between **4l**, **4m**, and **4n**. Compound **4g** containing no substituent on the phenyl ring at R^2 position showed the worst potency compared with those substituted by different groups (**4h**, **4i**, and **4j**). Variation of moieties at the R^3 position led to distinct activities. Replacement of aliphatic isopropyl group at the R^3 position of compound **4a** (136 nM) with aromatic phenyl (**4e**, 664 nM) or 4-methylphenyl ring (**4f**, 497 nM) respectively resulted in nearly 5-fold or 4-fold potency loss, which suggested that substituents at this position should be focused on aliphatic groups in the future drug design. And this is consistent with what had been discussed previously in dipeptidyl proteasome inhibitors composed of α-amino acids.

However, extensive understanding of SAR always requires a large sample size of inhibitors, as discussed in our

Table 1. Structures of Compounds **4a−q**, Bortezomib, and Their Inhibition of Human 20S Proteasome

compd	R^1	R^2	R^3	IC$_{50}$ (sd)^a, nM
4a	Pyz^b	H	^{i}Pr^c	136 (10.6)
4b	Pyz	CH$_3$	^{i}Pr	69.8 (8.6)
4c	Pyz	OCH$_3$	^{i}Pr	134 (17.7)
4d	Pyz	Cl	^{i}Pr	121 (15.1)
4e	Pyz	H	Ph	664 (66.6)
4f	Pyz	H	(4-CH$_3$)-Ph	497 (43.1)
4g	Ph	H	^{i}Pr	40 (5.3)
4h	Ph	CH$_3$	^{i}Pr	14 (1.7)
4i	Ph	OCH$_3$	^{i}Pr	12.5 (1.3)
4j	Ph	Cl	^{i}Pr	30 (4.4)
4k	nicotin-3-yl	H	^{i}Pr	382 (15.7)
4l	nicotin-3-yl	CH$_3$	^{i}Pr	165 (9.5)
4m	nicotin-3-yl	OCH$_3$	^{i}Pr	35 (4.6)
4n	nicotin-3-yl	Cl	^{i}Pr	180 (11.3)
4o	THNA^d	OCH$_3$	^{i}Pr	161 (15.9)
4p				350 (45.2)
4q				9.6 (1.3)
bortezomib				2.48^e (0.3)

^{a} Each IC$_{50}$ determination was performed with five concentrations, and each assay point was determined in duplicate. ^{b} Pyz, pyrazin-2-yl. ^{c} ^{i}Pr, iso-propyl. ^{d} THNA, 5,6,7,8-tetrahydronaphthalen-1-yl. ^{e} IC$_{50}$ value obtained for bortezomib under our experimental conditions.

dipeptidyl boronic acid proteasome inhibitors composed of α-amino acids.[16] Nowadays more structurally diverse compounds are being designed and synthesized to clearly and extensively elucidate the SAR so that much better candidates are obtained and developed.

Screening results showed that (±)-**4i** was the most active among all the racemates of dipeptidyl boronic acids. So we further investigated the activities of its two isomers **4p** and **4q**. Our studies showed that **4q** was 36-fold more active than its isomer **4p**, which suggested a strictly stereoselective mode of inhibition between such compounds and 20S proteasome, which is discussed later with a theoretical modeling method.

Cellular. The two isomers **4p** and **4q** and racemate (±)-**4i** showed quite different activities in inhibiting human 20S proteasome. How about the cellular activities of these isomers? Subsequently the cytotoxic potentials of compounds (±)-**4i**, **4p**, and **4q** were screened against 10 cell lines, including 2 human hematologic tumors, HL-60 (promyelocytic leukemia cell line) and U266 (multi myeloma cell line), and 8 solid tumors, BGC-823 (human gastric carcinoma cell line), H460 (human large cell lung cancer cell line), BXPC-3 (human pancreatic cancer cell line), SW-480 (human colon carcinoma cell line), A549 (human non-small-cell lung cancer cell line), PC-3 (human prostate cancer line), HepG2 (human hepatocellular liver carcinoma cell line), and SKOV-3 (human ovarian cancer cell line). The results are displayed in Table 2. All the three isomers showed good activities with IC$_{50}$ values nearly less than 5 μM against BXPC-3, SW-480, A549, PC-3, HepG2, HL-60, and U266 human cancer cell lines. Especially, such compounds were very sensitive to the two hematologic tumor cell lines, which was consistent with our previous results.[16] However, they were not so active against the other two BGC-823 and H460 human cancer cell lines. For most human cancer cell lines, the rank order of potency was **4q** > (±)-**4i** > **4p**. But the difference in cellular activities was not as large as in enzymatic assays.

Toxicity Assessment in Vivo. The zebrafish is rapidly gaining acceptance as a promising animal model for whole-organism screening for toxicology in the drug discovery process. Therefore, the compounds can be prioritized for further development.[34] In our candidates selection, the synthesized **4p**, **4q**, and bortezomib were screened using zebrafish embryos to evaluate their safety profiles in vivo. Interestingly, the two isomers, **4p** and **4q**, induced no morphological changes of the zebrafish embryos at 1 and 10 μmol concentrations in 24 h, which indicated both of the isomers were not toxic in vivo at this level. However, embryos treated with 1 and 10 μmol of bortezomib displayed different degrees of cell death in the body (Figure 1c and Figure 1d) and even embryos death (Figure 1b) compared with the control (Figure 1a). 28.5% of the embryos displayed cell death only in the tail (blue arrow indication, Figure 1c), while 52.4% of those showed a larger range of cell death in the whole embryo (blue arrow indication, Figure 1d). These facts indicated that the marketed bortezomib was potentially more toxic than the candidate **4q**, and the results of safety evaluation in Sprague−Dawley (SD) rats as discussed later also supported our supposition.

Pharmacokinetic Profiles and Toxicity of 4q. Up to now, no pharmacokinetic profiles were reported for dipeptidyl boronic acid proteasome inhibitors composed of β-amino acids. To evaluate the druggability of such compounds, the candidate **4q** was further investigated by profiling iv and ig pharmacokinetics in male SD rats. The results compared with bortezomib are illustrated in Table 3.

After iv bolus injection in male SD rats, **4q** was eliminated slowly with 2-fold longer time than bortezomib (elimination half-life $T_{1/2z}$ of 5.3 vs 2.0 h). Such a long elimination phase half-life is due in part to the larger volume of distribution (V_z = 8449 mL/kg) and much lower systemic clearance (CL$_z$ = 1126 (mL/h)/kg). Furthermore, area-under-the-curve (AUC) of **4q** reached 933 ng·h/mL, much larger than

Table 2. Cytotoxicity of Compounds against Tumor Cell Lines (IC$_{50}$, sd)[a]

compd	BGC-823	H460	BXPC-3	SW-480	A549	PC-3	SKOV-3	HepG2	HL-60	U266
4i (μM)	30.93(5.9)	36.0(6.4)	1.50(0.5)	1.08(0.29)	3.45(2.7)	0.83(0.2)	8.43(0.2)	5.59(0.3)	1.02(0.4)	2.65(0.2)
4p (μM)	76.86(7.6)	25.25(2.3)	2.82(2.4)	1.72(0.58)	3.68(2.2)	1.11(0.07)	14.5(0.4)	5.13(0.9)	0.70(0.3)	1.28(0.3)
4q (μM)	74.42(2.3)	14.60(0.7)	0.38(0.2)	0.41(0.12)	0.83(0.5)	0.23(0.04)	3.49(0.20)	1.88(0.1)	0.14(0.01)	0.35(0.04)
bortezomib (nM)[b]	3290(23.4)	780(13.3)	16.2(2.6)	6.1(0.4)	6.7(1.9)	7(7.6)	151(6.4)	7.5(0.7)	7.1(0.3)	8.8(0.43)

[a] Each cellular IC$_{50}$ determination was performed with 10 concentrations, and each assay point was determined in triplicate. [b] IC$_{50}$ value obtained for bortezomib under our experimental conditions.

Figure 1. Morphological changes of zebrafish embryos: (a) untreated embryo (24 h); (b) embryos treated with bortezomib (10 μmol, 24 h); (c, d) embryos treated with bortezomib (1 μmol, 24 h). Blue arrows indicate the region of cell death.

Table 3. Single Dose iv and ig Pharmacokinetic Profiles of **4q** and Bortezomib in SD Rats

compd	dose (mg/kg)	T_{max} (h)	C_{max} (ng/mL)	AUC$_{(0-t)}$ (ng·h/mL)	MRT$_{(0-t)}$ (h)	$T_{1/2z}$ (h)	V_z (mL/kg)	Cl$_z$ ((mL/h)/kg)
4q	1.0 iv	0.03	2929	933	2.8	5.3	8449	1126
	1.0 ig	ND[a]	ND[a]	ND[a]	ND[a]	ND[a]	ND[a]	ND[a]
bortezomib[b]	1.0 iv	0.03	1082	654	1.4	2.0	3744	1433
	1.0 ig	0.23	161	303	7.69	7.47	29791	2683

[a] ND: not detected. [b] All the data were obtained in our experimental conditions.

that of bortezomib (654 ng·h/mL), which suggested more plasma exposure in SD rats than in the standard.

However, when intragastrically administered in male SD rats, the concentration of **4q** declined below 5 ng/mL after half an hour in plasma, the lower limit of detection (LLOD). This lower oral bioavailability is possibly due to the declined absorption in the mouse gastrointestinal tract and first pass metabolism in the liver. However, the marketed bortezomib showed an approximate 46% oral bioavailability in our test. Though previous studies have shown that bortezomib was orally bioactive,[35,36] the current bortezomib therapy in multimyeloma and mantle cell lymphoma is still intravenous after being marketed for 6 years and no oral formulation was reported. Perhaps the instability of boronic acid pharmacophore in such proteasome inhibitors limits their development as oral formulation in clinical application.

After the pharmacokinetic experiment, the safety profiles of **4q** and bortezomib were compared. At 1.0 mg/kg iv and ig doses of bortezomib, all the SD rats died after 10 h, while the SD rats in **4q** group had not shown any toxic reactions. Nowadays, even at 2.0 mg/kg iv dose of **4q**, no any side

effects were observed. This result was consistent with what had been observed with the zebrafish. The detailed toxicity investigation and in vivo antitumor activities in human U266 and RPMI 8226 nude xenograft models will be reported elsewhere.

Docking Studies of 4p and 4q. Why were the enzymatic activities of isomers **4p** and **4q** quite different? Subsequently, docking studies were performed to try to theoretically explain it. To date, several ligand−proteasome crystal complexes have been reported.[37−40] On the basis of these experimental data, some theoretical modeling was carried out in different laboratories to describe the interaction mode between structurally diverse inhibitors and 20S proteasome.[41−45] However, the binding mode of dipeptidyl boronic acid composed of β-amino acid with catalytic β5 subunit had never been reported up to now. Because of the covalent binding of dipeptide boronic acid with proteasome, all the covalent docking processes were carried out by using GOLD, version 3.0,[46,47] which has a unique function to handle covalent docking.

First, to test the credibility of the developed docking procedure, the crystal structure of bortezomib was docked
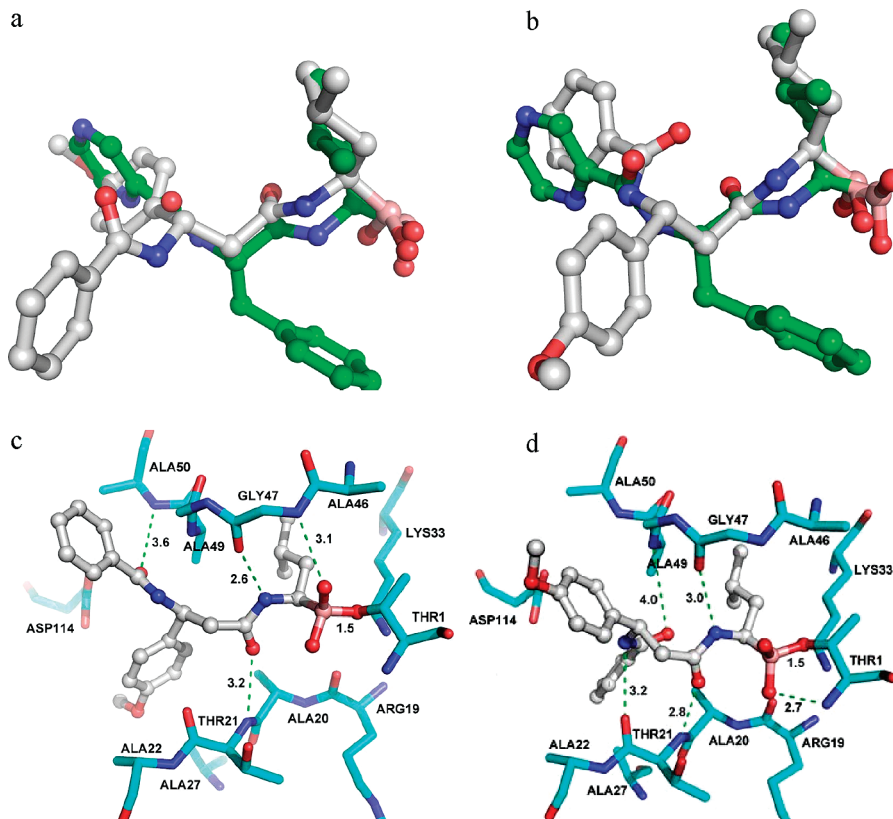
Figure 2. Alignment of **4p** and **4q** with bortezomib and their covalent docking results with β5 subunit: (a) alignment of **4p** (in gray) and bortezomib (in green); (b) alignment of **4q** (in gray) and bortezomib (in green); (c) binding mode of **4p** with β5 subunit; (d) binding mode of **4q** with β5 subunit. All the hydrogen atoms are not shown. The amino acid residues of β5 subunit are shown in stick models. **4p**, **4q**, and bortezomib are represented as ball and stick models. The picture were rendered in PyMOL, version 0.99.[48]

into the binding pocket of the β5 subunit. As shown by the docking results, the conformation with the highest fitness score produced by GOLD was closest to the crystal one, and the root-mean-square deviation (rmsd) of both conformations was only 2.0 Å, and the distances of covalent bond were 1.5 and 1.4 Å for docking conformation and crystal one. Orientations of the docked R^1, R^2, and R^3 substituents of bortezomib were quite similar to those of experimental one (Figure S1 of Supporting Information (SI)). Thus, the docking procedure was reliable enough to be used in the prediction of the binding modes of **4p**, **4q**, and 20S proteasome.

Analysis of docking results accounted for the different potency of the two isomers **4p** and **4q**. As demonstrated in Figure 2, the respective alignments of the two isomers **4p** (in gray, Figure 2a) and **4q** (in gray, Figure 2b) with bortezomib (in green, Figure 2a and Figure 2b) were quite different. R^3 substituents (isopropyl) of **4p** and bortezomib aligned quite well and oriented in the same direction. However, the R^2 group (p-methoxyphenyl) of **4p** wrongly overlapped with the R^1 substituent (pyrazin-2-yl) of bortezomib, while the R^1 group (benzoyl) of **4p** and R^2 one (phenyl) of bortezomib stretch to the same direction but with great deviation. For the case of **4q** and bortezomib, two substituents (R^1 and R^3) nearly overlapped; only the R^2 groups of both compounds deviated to a little extent. The more perfect alignment of **4q** than **4p** with bortezomib well explained the different activities in inhibiting 20S proteasome on the one hand.

On the other hand, detailed analysis of binding mode of **4p** and **4q** with active amino acid residues of β5 subunit also elucidated the inhibition variation. Figure 2c and Figure 2d respectively presented the interactions between **4p** and the β5

subunit and between **4q** and the β5 subunit. It showed that four strong and one weak H-bonds were formed between **4q** and amino acid residues of β5 subunit, while only three strong and one weak H-bonds were observed with **4p**. From docking results, C- and N-terminals of residue THR21 formed two H-bonds with **4q**, 3.2 and 2.8 Å length, respectively; however, **4p** formed only one 3.2 Å length H-bond with the N-terminal of this residue. Furthermore, one strong 2.7 Å length H-bond exists between the NH group of the catalytic THR1 residue and oxygen atom of boronic acid pharmacophore in **4q** in addition to a 1.5 Å length covalent bond.

In summary, the docking results offered us useful information for understanding the interaction mode and different potency between **4p** and **4q**. It is believed that theoretical docking can guide us to rationally design novel peptide boronic acid proteasome inhibitors in the future.

Conclusion

A series of dipeptidyl boronic acid proteasome inhibitors composed of β-amino acids were synthesized, biologically investigated in vitro and in vivo, and theoretically modeled. From these compounds, some structure−activity relationships were concluded and the enantiomer **4q** was identified as a stereoselective proteasome inhibitor at the nanomolar level, having nearly the same potency as the marketed bortezomib. But it was more potent than its isomer **4p** and racemic form (±)-**4i** in inhibiting 20S proteasome activity. Cellular assays substantially confirmed the activity of the compounds and were in line with the stereoselectivity interaction of the 20S

proteasome. In vivo toxicity assessment with zebrafish as a whole-organism screening showed that the two pure isomers were nontoxic while bortezomib induced some phenotypic changes to a certain extent, which was supported by observation of toxic reactions of SD rats after pharmacokinetic experiments. Pharmacokinetic profiles suggested that candidate **4q** showed a more plasma exposure and longer half-life than bortezomib. Docking studies indicated that **4q** adopted a similar mode to inhibit the 20S proteasome as bortezomib. The docking results offered us much useful information to understand the interaction mode between such inhibitors and 20S proteasome and will facilitate the next cycle of drug design.

Experimental Procedures

Commercially available reagents were used directly without any purification unless otherwise stated. Reaction progress was monitored by silica gel aluminum sheets (60F-254) and RP-18 F254s using UV light as a visualizing agent and 15% ethanolic phosphomolybdic acid and heat or ninhydrin and heat as developing agent. The 200−300 mesh silica gel and ODS C-18 were used for column chromatography. For compounds with fluorine atoms, analytical reverse phase HPLC was run using Sinochrom ODS-BP 4.6 mm × 150 mm column, eluting with a mixture of 20% acetonitrile and 80% water containing 1% β-cyclodextrin. For other compounds, a reverse phase Extend C18 4.6 mm × 150 mm column was employed and eluted with a mixture of 15% acetonitrile and 85% water containing 0.1% triethylamine. HPLC showed that the purity of all the final products was greater than 95%. Melting points were obtained on an YRT-3 melting point apparatus and were uncorrected. ^{1}H NMR and ^{13}C NMR spectra were recorded on Bruker Avance 300 or Avance 500 spectrometer with TMS as internal standard. Splitting patterns are described as singlet (s), doublet (d), triplet (t), quartet (q), broad (br), or doublet of doublet (dd). The value of chemical shifts (δ) is given in ppm and coupling constants (J) in Hertz (Hz). Mass spectra were obtained using Agilent LC−MS (1956B) instrument in electrospray positive and negative ionization modes. Mass spectra of product ions studied in pharmacokinetics were obtained using Agilent LC/MS/MS (6410). High-resolution mass spectra were recorded on a ZAB-HS instrument using an electrospray source (ESI).

The synthesis of chiral N-terminal protected β-amino acids **1p**, **1q**, intermediates **3i**, **3p**, **3q**, and target molecule **4i** and its two isomers **4p** and **4q** is indicated below. Detailed synthesis and structural characterization data of **1a−o**, **2a−q**, **3a−h**, **3j−o**, **4a−h**, and **4j−o** are described in Supporting Information.

(S)-3-Benzamido-3-(4-methoxyphenyl)propanoic Acid (1p). This compound was synthesized according to the reported methods. To a stirred solution of *tert*-butyl diethylphosphonoacetate (**8**) (0.44 g, 1.74 mmol) in absolute THF (3 mL) was dropwise added *n*-BuLi (0.7 mL, 2.5 M in hexane, 1.75 mmol) at −78 °C. After the mixture was stirred for 2 h at −78 °C, a solution of the aldehyde (0.17 g, 1.74 mmol) in THF (2 mL) was added all at once. The resulting solution was stirred at −78 °C for 3 h before rising to room temperature. The solution was subsequently cooled to −78 °C and quenched with saturated aqueous NH$_4$Cl (2 mL). THF was removed in vacuo. The product was extracted with DCM (3 × 15 mL), the combined organic extracts were dried with anhydrous Na$_2$SO$_4$, and the solvent was removed in vacuo to yield the crude product, which was chromatographed using CH$_2$Cl$_2$/petroleum (1:20) as eluent to give a pure sticky solid (**9**) (0.30 g, 86%). ^{1}H NMR (CDCl$_3$, 300 MHz) δ 1.53 (−CH$_3$, m, 9H), 3.83 (−OCH$_3$, s, 3H), 6.24 (−C=CH, d, J = 15.9 Hz, 1H), 6.87−6.90 (−Ph, m, 2H), 7.44−7.47 (−Ph, m, 2H), 7.54 (−C=CH, d, J = 15.9 Hz, 1H). MS (ESI) m/z 257.0 [M + Na]$^+$.

To a stirred solution of (*R*)-N-benzyl-N-α-methylbenzylamine (0.19 g, 0.9 mmol) in THF (3 mL) was slowly added

n-BuLi (0.4 mL, 2.5 M in hexane, 1 mmol) at −78 °C. After 1 h, a solution of α,β-unsaturated ester (**9**) (0.1 g, 0.5 mmol) in THF (2 mL) was added all at once. The resulting solution was stirred at −78 °C for 4 h before quenching with saturated aqueous NH$_4$Cl (1 mL). When the mixture was warmed to room temperature, THF was removed and the product was extracted with DCM. The organic fractions were washed with 10% aqueous nitric acid, saturated aqueous sodium bicarbonate, and brine and dried over anhydrous Na$_2$SO$_4$ and the solvent was removed in vacuo to yield the crude product, which was chromatographed using ethyl acetate/petroleum (1:50) as eluent to give pure pale-yellow **11a** (0.20 g, 88.4%). ^{1}H NMR (CDCl$_3$, 500 MHz) δ 1.19−1.25 (−CH$_3$, m, 12H), 2.46 (−CH$_2$, dd, J_1 = 10.2 Hz, J_2 = 14.5 Hz, 1H), 2.52 (−CH$_2$, dd, J_1 = 4.9 Hz, J_2 = 14.5 Hz, 1H), 3.66 (−CH$_2$, s, 2H), 3.78 (−OCH$_3$, s, 3H), 3.98 (−CH, q, J = 6.8 Hz, 1H), 4.34 (−CH, q, J = 4.9 Hz, 1H), 6.84−6.86 (−Ph, m, 2H), 7.14−7.15 (−Ph, m, 1H), 7.20−7.25 (−Ph, m, 4H), 7.28−7.31 (−Ph, m, 4H), 7.39−7.41 (−Ph, m, 2H). ^{13}C NMR (CDCl$_3$, 125 MHz) δ 27.76, 38.57, 55.16, 57.10, 59.09, 60.31, 80.04, 126.45, 126.70, 127.79, 127.99, 128.09, 128.15, 129.33, 133.90, 141.86, 144.36, 158.68, 171.19. MS (ESI) m/z 446.2 [M + H]$^+$, 468.2 [M + Na]$^+$.

To a stirred solution of **11a** (0.88 g, 1.98 mmol) in methanol (6 mL), distilled water (0.7 mL), and acetic acid (0.2 mL) was added palladium hydroxide on carbon (1 g, 64.3% water). A hydrogen balloon was attached and the resulting suspension stirred for 24 h under 1 atm of hydrogen. The reaction mixture was filtered through Celite, and the solvent was removed in vacuo. The residue was partitioned between DCM (10 mL) and saturated aqueous NaHCO$_3$ (5 mL). The organic phase was separated, and the aqueous phase was extracted with DCM (2 × 10 mL). The combined organic layers were dried over Na$_2$SO$_4$, and the solvent was removed in vacuo. The residue was crudely purified by passing through a short plug of silica gel (DCM/ Et$_3$N 100:1) to yield the product **12a** (0.64 g, 73.4%), which was directly used in the next reaction.

At 0 °C, to a stirred solution of **12a** (0.60 g, 2.40 mmol) and NMM (0.30 g, 2.97 mmol) in THF (10 mL) was added benzoyl chloride (0.4 g, 2.85 mmol). The mixture was allowed to stir overnight. The solvent was evaporated and dissolved in DCM (20 mL), washed with 10% nitric acid, saturated aqueous NaHCO$_3$ (10 mL), and brine, and dried over anhydrous Na$_2$SO$_4$. The solvent was removed in vacuo, and the residue was dissolved in HCl/Et$_2$O (10 mL, 6M, 60 mmol) and stirred overnight at 0 °C. The organic phase was removed in vacuo and the resulting solid was washed with ether (3 × 10 mL) and dried to give the title compound **1p** (0.21 g, 58.6%) as a white solid. Chiral HPLC indicated purity of 100 area %, and no isomer was detected. Mp 175.7−176.9 °C. ^{1}H NMR (DMSO-d_6, 500 MHz) δ 2.75 (−CH$_2$, dd, J_1 = 6.2 Hz, J_2 = 15.4 Hz, 1H), 2.88 (−CH$_2$, dd, J_1 = 6.9 Hz, J_2 = 15.5 Hz, 1H), 3.72 (−CH$_3$, s, 3H), 5.39 (−CH, dd, J_1 = 6.8 Hz, J_2 = 8.1 Hz, 1H), 6.87−6.89 (−Ph, m, 2H), 7.33−7.34 (−Ph, m, 2H), 7.44−7.47 (−Ph, m, 2H), 7.50−7.53 (−Ph, m, 1H), 7.83−7.84 (−Ph, m, 2H), 8.79 (−CONH, d, J = 8.2 Hz, 1H), 12.20 (−COOH, s, 1H). ^{13}C NMR (DMSO-d_6, 125 MHz) δ 49.38, 54.97, 113.55, 127.17, 127.66, 128.09, 131.04, 134.44, 134.68, 158.14, 165.30, 171.76. MS (ESI) m/z 299.3 [M − H]$^-$.

(R)-3-Benzamido-3-(4-methoxyphenyl)propanoic Acid (1q). Compound **1q** was prepared in 61.6% yield following a similar procedure described for the synthesis of **1p**. Chiral HPLC indicated purity of 100 area %, and no isomer was detected.

Synthesis of 11b. The synthesis involved (*S*)-N-Benzyl-N-α-methylbenzylamine (0.38 g, 1.8 mmol), *n*-BuLi (0.8 mL, 2.5 M in hexane, 2.0 mmol), and α,β-unsaturated ester (**9**) (0.23 g, 1.0 mmol), giving 85% yield. ^{1}H NMR (CDCl$_3$, 500 MHz) δ 1.19−1.25 (−CH$_3$, m, 12H), 2.46 (−CH$_2$, dd, J_1 = 10.2 Hz, J_2 = 14.4 Hz, 1H), 2.52 (−CH$_2$, dd, J_1 = 5.0 Hz, J_2 = 14.4 Hz, 1H), 3.66 (−CH$_2$, s, 2H), 3.78 (−OCH$_3$, s, 3H), 3.98 (−CH, q, J = 6.8 Hz, 1H), 4.34 (−CH, q, J = 5.0 Hz, 1H), 6.84−6.86 (−Ph, m,

2H), 7.14−7.17 (−Ph, m, 1H), 7.19−7.27 (−Ph, m, 5H), 7.28−7.31 (−Ph, m, 4H), 7.39−7.41 (−Ph, m, 2H). ^{13}C NMR (CDCl$_3$, 125 MHz) δ 27.76, 38.57, 55.16, 57.10, 59.09, 60.31, 80.04, 126.45, 126.76, 127.79, 127.81, 128.09, 128.15, 129.33, 133.90, 141.86, 144.36, 158.68, 171.19. MS (ESI) *m/z* 446.2 [M + H]$^+$.

Synthesis of 12b. To compound (**11b**) (0.35 g, 0.78 mmol), methanol (5 mL), distilled water (0.5 mL), and acetic acid (0.1 mL) was added palladium hydroxide on carbon (0.4 g, 64.3% water). Purification with chromatography (CH$_2$Cl$_2$ as eluent) gave a yellow oil **12b** (0.17 g, 89.2%).

Synthesis of 1q. The synthesis involved compound **12b** (0.1 g, 0.4 mmol), NMM (0.05 mL, 0.48 mmol), benzoyl chloride (0.06 mL, 0.48 mmol), and HCl/Et$_2$O (5 mL, 6 M, 30 mmol), giving 61.6% yield. Mp 183.5−186.7 °C. ^{1}H NMR (DMSO-d_6, 500 MHz) δ 2.75 (−CH$_2$, dd, J_1 = 6.5 Hz, J_2 = 15.6 Hz, 1H), 2.88 (−CH$_2$, dd, J_1 = 8.7 Hz, J_2 = 15.6 Hz, 1H), 3.72 (−CH$_3$, s, 3H), 5.39 (−CH, dd, J_1 = 6.6 Hz, J_2 = 8.4 Hz, 1H), 6.87−6.89 (−Ph, m, 2H), 7.32−7.35 (−Ph, m, 2H), 7.44−7.47 (−Ph, m, 2H), 7.50−7.53 (−Ph, m, 1H), 7.82−7.84 (−Ph, m, 2H), 8.79 (−CONH, d, J = 8.3 Hz, 1H), 12.12 (−COOH, s, 1H). ^{13}C NMR (DMSO-d_6, 125 MHz) δ 49.42, 54.98, 113.58, 127.21, 127.70, 128.12, 131.07, 134.48, 134.73, 158.18, 165.34, 171.80. MS (ESI) *m/z* 299.3.

Pinanediol Ester (R)-1-[3-Benzamido-3-(4-methoxyphenyl)-propanamido]-3- methylbutylboronic Acid (3i). To a cooled solution (−5 °C) of 3-benzamido-3-(4-methoxy)phenylpropanoic acid (**1i**) (0.21 g, 0.70 mmol) dissolved in anhydrous CH$_2$Cl$_2$ (15 mL) was added HOBt (0.23 g, 1.70 mmol). After 20 min, the reaction system was cooled to −15 °C and EDC·HCl (0.33 g, 1.70 mmol) was added. Finally the precooled (0 °C) mixture of the known pinanediol boronate aminohydrochloride (**2i**) (0.21 g, 0.70 mmol) and DIPEA (0.15 mL, 0.84 mmol) in anhydrous CH$_2$Cl$_2$ (10 mL) was poured. The mixture was stirred at −15 °C for 1 h and at room temperature for 2 h, and the reaction was finally quenched with water. The aqueous phase was extracted with CH$_2$Cl$_2$ (3 × 100 mL). The combined organic phase was washed with 10% citric acid, 5% NaHCO$_3$, and brine, dried over anhydrous Na$_2$SO$_4$, filtered, and evaporated to provide crude product **3i**, which was directly used in the next reaction.

Pinanediol Ester (R)-1-[(S)-3-Benzamido-3-(4-methoxyphenyl)-propanamido]-3-methylbutylboronic Acid (3p). The synthesis involved a similar procedure as above but with **1p** (0.27 g, 1.00 mmol), CH$_2$Cl$_2$ (30 mL), HOBt (0.16 g, 1.20 mmol), EDC·HCl (0.19 g, 1.00 mmol), **2p** (0.30 g, 1.00 mmol), DIPEA (0.26 mL, 1.48 mmol). After being washed with 10% citric acid, 5% NaHCO$_3$, and brine and dried over anhydrous Na$_2$SO$_4$, the crude product was directly used in the next reaction.

Pinanediol Ester (R)-1-[(R)-3-Benzamido-3-(4-methoxyphenyl)-propanamido]-3-methylbutylboronic Acid (3q). The synthesis involved a similar procedure as above but with **1q** (0.27 g, 1.00 mmol), CH$_2$Cl$_2$ (50 mL), HOBt (0.16 g, 1.20 mmol), EDC·HCl (0.19 g, 1.00 mmol), **2q** (0.30 g, 1.00 mmol), DIPEA (0.26 mL, 1.48 mmol). After being washed with 10% citric acid, 5% NaHCO$_3$, and brine and dried over anhydrous Na$_2$SO$_4$, the crude product was directly used in the next reaction.

(R)-1-[3-Benzamido-3-(4-methoxyphenyl)propanamido]-3-methylbutylboronic Acid (4i). To a solution of **3i** (0.35 g, 0.64 mmol) and 2-methylpropylboronic acid (0.33 g, 3.20 mmol) dissolved in methanol (13 mL) and hexane (13 mL) was added 1 N HCl (1.6 mL). The mixture was stirred at room temperature for 18 h. The methanolic phase was washed with hexane (3 × 10 mL), and the hexane layer was extracted with methanol (3 × 15 mL). The combined methanolic layers were evaporated in vacuo, and the residue was dissolved in CH$_2$Cl$_2$ (30 mL). The solution was washed with 5% NaHCO$_3$ (15 mL), and the organic layer was dried over anhydrous Na$_2$SO$_4$, evaporated, and purified with chromatography (CH$_3$OH/CH$_2$Cl$_2$ = 1:20 and then 1:5) to obtain 190 mg (71.3% yield) of a pale-yellow foam solid **4i**. ^{1}H NMR (CD$_3$OD, 300 MHz) δ 0.83−0.89 (−CH$_3$, m, 6H),

1.23−1.31 (−CH$_2$, m, 2H), 1.46−1.59 (−CH, m, 1H), 2.58 (−CH, t, J = 7.9 Hz, 1H), 2.98−3.07 (−CH$_2$, m, 2H), 3.77 (−CH$_3$, s, 3H), 5.58 (−CH, t, J = 7.8 Hz, 1H), 6.90 (−Ph, d, J = 8.6 Hz, 2H), 7.36−7.39 (−Ph, m, 2H), 7.42−7.47 (−Ph, m, 2H), 7.51−7.56 (−Ph, m, 1H), 7.80−7.82 (−Ph, m, 2H). ^{13}C NMR (CD$_3$OD, 75 MHz) δ 22.11, 23.86, 26.88, 37.72, 41.02, 51.67, 55.76, 115.16, 128.42, 128.97, 129.52, 132.78, 135.60, 160.83, 169.55, 177.07. MS (ESI) *m/z* 440.2 [M + 2CH$_2$]$^-$, 450.2 [M + 37]$^+$. HRMS [M + Na + 2CH$_2$]$^+$ calcd, 463.2380; found, 463.2409.

(R)-1-[(S)-3-Benzamido-3-(4-methoxyphenyl)propanamido]-3-methylbutylboronic Acid (4p). The synthesis involved a similar procedure as described for **4i**, using **3p** (0.55 g, 1.00 mmol), 2-methylpropylboronic acid (0.51 g, 5.0 mmol), methanol (15 mL), hexane (15 mL), 1 N HCl (2.5 mL) to give 0.22 g of a white foam solid (53.3% yield). ^{1}H NMR (CD$_3$OD, 500 MHz) δ 0.84−0.88 (−CH$_3$, m, 6H), 1.14−1.17 (−CH$_2$, m, 1H), 1.23−1.25 (−CH$_2$, m, 1H), 1.50−1.58 (−CH, m, 1H), 2.58 (−CH, dd, J_1 = 8.6 Hz, J_2 = 6.5 Hz, 1H), 3.02−3.13 (−CH$_2$, m, 2H), 3.77 (−CH$_3$, s, 3H), 5.57 (−CH, t, J = 7.8 Hz, 1H), 6.91 (−Ph, d, J = 8.7 Hz, 2H), 7.37 (−Ph, d, J = 8.7 Hz, 2H), 7.43−7.46 (−Ph, m, 2H), 7.51−7.54 (−Ph, m, 1H), 7.80−7.82 (−Ph, m, 2H). ^{13}C NMR (CD$_3$OD, 125 MHz) δ 21.98, 23.88, 26.87, 37.82, 41.01, 45.60, 51.67, 55.75, 115.18, 128.50, 129.12, 129.58, 132.85, 133.77, 135.64, 160.93, 169.69, 177.22. MS (ESI) *m/z* 448.2 [M + Cl]$^-$, 435.1 [M + Na]$^+$. HRMS [M + Na + 2CH$_2$]$^+$ calcd, 463.2379; found, 463.2371.

[(1R)-1-[[(3R)-3-(4-Methoxyphenyl)-3-[(phenylcarbonyl)amino]-1-oxopropyl]amino]-3-methylbutyl]boronic Acid (4q). The synthesis involved a similar procedure as described for **4i**, using **3q** (0.55 g, 1.00 mmol), 2-methylpropylboronic acid (0.51 g, 5.0 mmol), methanol (20 mL), hexane (20 mL), 1 N HCl (2.5 mL) to give 0.232 g of a white foam solid (56.4% yield). ^{1}H NMR (CD$_3$OD, 500 MHz) δ 0.83−0.88 (−CH$_3$, m, 6H), 1.15−1.17 (−CH$_2$, m, 1H), 1.22−1.26 (−CH$_2$, m, 1H), 1.51−1.58 (−CH, m, 1H), 2.58 (−CH, q, J = 6.5 Hz, 1H), 3.04 (−CH$_2$, dd, J_1 = 5.6 Hz, J_2 = 14.6 Hz, 1H), 3.10 (−CH$_2$, dd, J_1 = 8.4 Hz, J_2 = 14.6 Hz, 1H), 3.77 (−OCH$_3$, s, 3H), 5.57 (−CH, t, J = 7.9 Hz, 1H), 6.89−6.92 (−Ph, m, 2H), 7.36−7.38 (−Ph, m, 2H), 7.43−7.46 (−Ph, m, 2H), 7.51−7.54 (−Ph, m, 1H), 7.80−7.82 (−Ph, m, 2H). ^{13}C NMR (CD$_3$OD, 125 MHz) δ 22.09, 23.83, 26.98, 37.67, 45.61, 48.49, 51.58, 55.75, 128.46, 129.08, 129.56, 132.82, 133.74, 135.60, 160.86, 169.59, 177.21. MS (ESI) *m/z* 435.1 [M + Na]$^+$. HRMS [M + Na + 2CH$_2$]$^+$ calcd, 463.2379; found, 463.2371.

Enzyme and Inhibition Asssays. The 20S proteasome activity assay kit was purchased from Chemicon. Other reagents and solvents were purchased from commercial sources. In brief, substrates and compounds were previously dissolved in DMSO, with the final solvent concentration kept constant at 3% (v/v). The reaction buffers were (pH 7.5) 20 mM Tris, 1 mM DTT, 10% glycerol, and 0.02% (w/v) DS for CT-L activities. Proteasome activity was determined by monitoring the hydrolysis of the fluorogenic substrate, Suc-Leu-Leu-Val-Tyr-AMC (λ_{exc} = 360 and λ_{exc} = 465 nm for AMC substrates), reacting for 1 h at 37 °C in the presence of untreated (control) or proteasome that had been incubated with five different concentrations of test compounds. Fluorescence was measured using an Infinite M200 microplate reader (Tecan, Austria).

Cell Culture and Cytotoxicity Assays. HL-60 (promyelocytic leukemia cell line), BXPC-3 (human pancreatic cancer cell line), PC-3 (human prostate cancer line), and U266 (multimyeloma cell line) human cell lines were obtained from the American Type Culture Collection (Manassas, VA). H460 (human large cell lung cancer cell line), A549 (human nonsmall cell lung cancer cell line), SW-480 (human colon carcinoma cell line), SKOV-3 (human ovarian carcinoma), HepG2 (human hepatocellular liver carcinoma cell line), and BGC-823 (human gastric carcinoma cell line) cell lines were obtained from China Pharmaceutical University. HL-60 cell was cultured in IMDM

supplemented with 20% fetal bovine serum at 37 °C in 5% CO_2. BGC-823, BXPC-3, H460, HepG2, and SW-480 cells were grown in RPMI 1640 supplemented with 10% fetal bovine serum at 37 °C in 5% CO_2. U266 cell was cultured in RPMI 1640 supplemented with 15% fetal bovine serum at 37 °C in 5% CO_2. PC-3 and A549 cells were cultured in F12-k supplemented with 10% fetal bovine serum at 37 °C in 5% CO_2. SKOV-3 cell was cultured in McCoy's 5A supplemented with 10% fetal bovine serum at 37 °C in 5% CO_2.

A standard MTT assay was used to measure cell growth. In brief, a suspension of 3000 cells/150 μL of medium was added to each well of 96-well plates and allowed to grow. Twenty-four hours later, drugs prepared in medium at 10 different concentrations were added to the corresponding plates at a volume of 50 μL per well, and the plates were incubated for 72 h with drugs. Then an amount of 20 μL of a solution of 5 mg/mL MTT was added to each well and incubated for another 4 h at 37 °C. Plates were then centrifuged at 1000 rpm at 4 °C for 5 min, and the medium was carefully discarded. The formazan crystals were dissolved in 100 μL of DMSO, and absorbance was read on an Infinite M200 (Tecan, Austria) microplate reader at 540 nm. The result was expressed as the mean IC_{50} value, which is the average from at least three independent determinations.

Zebrafish Screening. AB strain was used in the experiment. Embryos were fed in Holtfreter's water at 28.5 °C and staged according to Kimmel et al.[49] The stock was made by dissolving test compounds first in absolute ethanol and then diluted in Holtfreter's water to a concentration of 0.01 M, while the concentration of absolute ethanol was kept at 1%. The stock was stored at −20 °C and diluted to a working concentration in Holtfreter's water. Embryos were treated from bud stage in the solution of test compounds and observed afterward and photographed at 24 h postfertilization (hpf) using a Leica MZ 16 stereomicroscope.

Pharmacokinetic Analyses in Rodents. Solutions of **4q** and bortezomib were prepared in 1% ethanol, 1% Tween-80, and 98% buffered saline with the final concentration of both compounds being 0.5 mg/mL for iv and ig administration. Heparinized blood samples collected for PK analyses ($n = 4$) were centrifuged at 4000 rpm for 5 min at 4 °C. Plasma samples were analyzed after protein precipitation with acetonitrile acidified with 1% formic acid. LC/MS/MS analysis of **4q** and bortezomib was performed under optimized conditions to obtain the best sensitivity and selectivity of the analyte in selected reaction monitoring mode (SRM). Selected product ions of **4q** were monitored for the quantification of the compound using bortezomib as an internal standard. Plasma concentration−time data were analyzed by a noncompartmental approach using the software WinNonlin Enterprise, version 5.2 (Pharsight Co., Mountain View, CA).

Docking Studies. The protein and ligands for docking were prepared using the software Insight II.[50] The initial structure of bortezomib was derived from the crystal complex coordinates (PDB code 2F16), and the original structures of **4p** and **4q** were constructed on the basis of the bortezomib crystal structure conformation followed by energy minimization. **4p** and **4q** were then covalently docked to the binding pocket of β5 subunit using GOLD, version 3.0. A radius of 20 Å from the β5 catalytic N-terminal threonine was used to direct site location. For each of the genetic algorithm runs, a maximum of 100 000 operations were performed on a population of 100 individuals with a selection pressure of 1.1. Operator weights for crossover, mutation, and migration were set to 95, 95, and 10, respectively, as recommended by the authors of the software. Fifty GA runs were performed in each docking experiment as done in the software validation procedure. The default GOLD fitness function was used to identify the better binding mode.[51] The distance for hydrogen bonding was set to 2.5 Å, and the cutoff value for van der Waals calculation was set to 4 Å. Covalent docking was applied, and the terminal boron atoms of all the ligands were bonded to the hydroxyl oxygen of Thr1.

Supporting Information Available: General and experimental procedures; characterization data for **1a−o**, **2a−q**, **3a−h**, **3j−o**, **4a−h**, **4j−o**; and comparison of binding mode between docked and crystal bortezomib. This material is available free of charge via the Internet at http://pubs.acs.org.

References

(1) Goldberg, A. L. Protein degradation and protection against misfolded or damaged proteins. *Nature* **2003**, *426*, 895–899.

(2) Ciechanover, A. The ubiquitin proteolytic system: from a vague idea, through basic mechanisms, and onto human diseases and drug targeting. *Neurology* **2006**, *66*, S7–S19.

(3) Ciechanover, A. The ubiquitin−proteasome pathway: on protein death and cell life. *EMBO J.* **1998**, *17*, 7151–7160.

(4) Malik, B.; Price, S. R.; Mitch, W. E.; Yue, Q.; Eaton, D. C. Regulation of epithelial sodium channels by the ubiquitin-proteasome proteolytic pathway. *Am. J. Physiol.: Renal Physiol.* **2006**, *290*, F1285–F1294.

(5) Nalepa, G.; Rolfe, M.; Harper, J. W. Drug discovery in the ubiquitin−proteasome system. *Nat. Rev. Drug Discovery* **2006**, *5*, 596–613.

(6) Voges, D.; Zwickl, P.; Baumeister, W. The 26S proteasome: a molecular machine designed for controlled proteolysis. *Annu. Rev. Biochem.* **1999**, *68*, 1015–1068.

(7) Adams, J. The development of proteasome inhibitors as anticancer drugs. *Cancer Cell* **2003**, *5*, 417–421.

(8) Orlowski, R. Z.; Zeger, E. L. Targeting the proteasome as a therapeutic strategy against hematological malignancies. *Expert Opin. Invest. Drugs* **2006**, *15*, 117–130.

(9) Townsend, A. R.; Millward, M.; Price, T.; Mainwaring, P.; Spencer, A.; Longenecker, A.; Palladino, M. A.; Lloyd, G. K.; Spear, M. A.; Padrik, P. Clinical trial of NPI-0052 in advanced malignancies including lymphoma and leukemia (advanced malignancies arm). *J. Clin. Oncol.* **2009**, *27*, 3582.

(10) Papandreou, C. N.; Daliani, D. D.; Nix, D.; Yang, H.; Madden, T.; Wang, X.; Pien, C. S.; Millikan, R. E.; Tu, S. M.; Pagliaro, L.; Kim, J.; Adams, J.; Elliott, P.; Esseltine, D.; Petrusich, A.; Dieringer, P.; Perez, C.; Logothetis, C. J. Phase I trial of the proteasome inhibitor bortezomib in patients with advanced solid tumors with observations in androgen-independent prostate cancer. *J. Clin. Oncol.* **2004**, *22*, 2108–2121.

(11) Cusack, J. C. Rationale for the treatment of solid tumors with the proteasome inhibitor bortezomib. *Cancer Treat Rev.* **2003**, *29* (Suppl. 1), 21–31.

(12) Chauhan, D.; Hideshima, T.; Anderson, K. C. Proteasome inhibition in multiple myeloma: therapeutic implication. *Annu. Rev. Pharmacol. Toxicol.* **2005**, *45*, 465–476.

(13) Zhu, Y. Q.; Pei, J. F.; Liu, Z. M.; Lai, L. H.; Cui, J. R.; Li, R. T. 3D-QSAR studies on tripeptide aldehyde inhibitors of proteasome using CoMFA and CoMSIA methods. *Bioorg. Med. Chem.* **2006**, *14*, 1483–1496.

(14) Zhu, Y. Q.; Lei, M.; Lu, A. J.; Zhao, X.; Yin, X. J.; Gao, Q. Z. 3D-QSAR studies of boron-containing dipeptides as proteasome inhibitors with CoMFA and CoMSIA methods. *Eur. J. Med. Chem.* **2009**, *44*, 1486–1499.

(15) Zhu, Y. Q.; Yao, S. Y.; Xu, B.; Ge, Z. M.; Cui, J. R.; Chen, T. M.; Li, R. T. Design, synthesis and biological evaluation of tripeptide boronic acid proteasome inhibitors. *Bioorg. Med. Chem.* **2009**, *17*, 6851–6861.

(16) Zhu, Y. Q.; Zhao, X.; Zhu, X. R.; Wu, G.; Li, Y. J.; Ma, Y. H.; Yuan, Y. X.; Yang, J.; Hu, Y.; Ai, L.; Gao, Q. Z. Design, synthesis, biological evaluation, and structure−activity relationship (SAR) discussion of dipeptidyl boronate proteasome inhibitors, part I: comprehensive understanding of the SAR of α-amino acid boronates. *J. Med. Chem.* **2009**, *52*, 4192–4199.

(17) Seebach, D.; Abele, S.; Schreiber, J. V.; Martinoni, B.; Nussbaum, A. K.; Schild, H.; Schulz, H.; Henneke, H.; Woessner, R.; Bitsch, F. Biological and pharmacokinetic studies with β-peptides. *Chimia* **1998**, *52*, 734–739.

(18) Shinagawa, S.; Kanamaru, T.; Harada, S.; Asai, M.; Okazaki, H. Chemistry of emeriamine and its analogs and their inhibitory activity in long-chain fatty acid oxidation. *J. Med. Chem.* **1987**, *30*, 1458–1463.

(19) Borman, S. β-Peptide: nature improved? *Chem. Eng. News* **1997**, *75*, 32–35.

(20) Seebach, D.; Abele, S.; Gademann, K.; Guichard, G.; Hintermann, T.; Jaun, B.; Mattews, J. L.; Schreiber, J. V.; Oberer, L.; Hommel, U.; Widmer, H. β²- and β³-peptides with proteinaceous side chains: synthesis and solution structures of constitutional isomers, a novel helical secondary structure and the influence of solvation and hydrophobic interactions on folding. *Helv. Chim. Acta* **1998**, *81*, 932–982.

(21) Appella, D. H.; Barchi, J. J., Jr.; Durell, S. R.; Gellman, S. H. Formation of short, stable helices in aqueous solution by β-amino acid hexamers. *J. Am. Chem. Soc.* **1999**, *121*, 2309–2310.

(22) Hanessian, S.; Yang, H. Design of a novel secondary structure scaffolding device: induction of a reverse turn in tetrapeptides by incorporating a β-amino acid and stereocontrolled free radical α-substitution reactions in peptide motifs. *Tetrahedron Lett.* **1997**, *38*, 3155–3158.

(23) Langheinrich, U. Zebrafish: a new model on the pharmaceutical catwalk. *BioEssays* **2003**, *25*, 904–912.

(24) Milan, D. J.; Peterson, T. A.; Ruskin, J. N.; Peterson, R. T.; MacRae, C. A. Drugs that induce repolarization abnormalities cause bradycardia in zebrafish. *Circulation* **2003**, *107*, 1355–1358.

(25) Zon, L. I.; Peterson, R. T. In vivo drug discovery in the zebrafish. *Nat. Rev. Drug Discovery* **2005**, *4*, 35–44.

(26) McGraph, P.; Li, C. Q. Zebrafish: a predictive model for assessing drug-induced toxicity. *Drug Discovery Today* **2008**, *13*, 394–401.

(27) Parng, C. In vivo zebrafish assays for toxicity testing. *Curr. Opin. Drug Discovery Dev.* **2005**, *8*, 100–106.

(28) Murtha, J. M.; Qi, W.; Keller, E. T. Hematologic and serum biochemical values for zebrafish (*Danio rerio*). *Comp. Med.* **2003**, *53*, 37–41.

(29) Parng, C.; Roy, N. M.; Ton, C.; Lin, Y.; McGrath, P. Neurotoxicity assessment using zebrafish. *J. Pharmacol. Toxicol. Methods* **2007**, *55*, 103–112.

(30) Amanuma, K.; Takeda, H.; Amanuma, H.; Aoki, Y. Transgenic zebrafish for detecting mutations caused by compounds in aquatic environments. *Nat. Biotechnol.* **2000**, *18*, 62–65.

(31) Klausner, Y. S.; Bodansky, M. Coupling reagents in peptide synthesis. *Synthesis* **1972**, 453–463.

(32) Davies, S. G.; Hermann, G. J.; Sweet, M. J.; Smith, A. D. Double asymmetric induction as a mechanistic probe: conjugate addition for the asymmetric synthesis of a pseudotripeptide. *Chem. Commun.* **2004**, 1128–1129.

(33) Davies, S. G.; Mulvaney, A. W.; Russell, A. J.; Smith, A. D. Parallel synthesis of homochiral β-amino acids. *Tetrahedron: Asymmetry* **2007**, *18*, 1554–1566.

(34) Spitsbergen, J. M.; Kent, M. L. The state of the art of the zebrafish model for toxicology and toxicologic pathology research—advantages and current limitations. *Toxicol. Pathol.* **2003**, *31* (Suppl.), 62–87.

(35) Pallombella, V. J.; Conner, E. M.; Fuseler, J. W.; Destree, A.; Davis, J. M.; Laroux, F. S.; Wolf, R. E.; Huang, J.; Brand, S.; Elliott, P. J.; Lazarus, D.; Parent, L.; Stein, R.; Adams, J.; Grisham, M. B. Role of the proteasome and NF-kappa B in streptoccal cell wall-induced polyarthritis. *Proc. Natl. Acad. Sci. U.S.A.* **1998**, *95*, 15671–15676.

(36) Teicher, B. A.; Ara, G.; Herbst, R.; Palombella, V. J.; Adams, J. The proteasome inhibitor PS-341 in cancer therapy. *Clin. Cancer Res.* **1999**, *5*, 2638–2645.

(37) Löwe, J.; Stock, D.; Jap, B.; Zwickl, P.; Baumeister, W.; Huber, R. Crystal structure of the 20S proteasome from the archaeon *T. acidophilum* at 3.4 Å resolution. *Science* **1995**, *268*, 533–539.

(38) Groll, M.; Ditzel, L.; Löwe, J.; Stock, D.; Bochtler, M. B.; Huber, R. Structure of 20S proteasome from yeast at 2.4 Å resolution. *Nature (London)* **1997**, *386*, 463–471.

(39) Groll, M.; Huber, R.; Potts, B. C. M. Crystal structures of salinosporamide A (NPI-0052) and B (NPI-0047) in complex with the 20S proteasome reveal important consequences of β-lactone ring opening and mechanism for irreversible binding. *J. Am. Chem. Soc.* **2006**, *128*, 5136–5141.

(40) Groll, M.; Berkers, C. R.; Ploegh, H. L.; Ovaa, H. Crystal structure of the boronic acid-based proteasome inhibitor bortezomib in complex with the yeast 20S proteasome. *Structure* **2006**, *14*, 451–456.

(41) Furet, P.; Imbach, P.; Fürst, P.; Lang, M.; Noorani, M.; Zimmermann, J.; García-Echeverría, C. Modeling of the binding mode of a non-covalent inhibitor of the 20S proteasome. Application to structure-based analogue design. *Bioorg. Med. Chem. Lett.* **2001**, *11*, 1321–1324.

(42) Smith, D. M.; Daniel, K. G.; Wang, Z. G.; Guida, W. C.; Chan, T. H.; Dou, Q. P. Docking studies and model development of tea polyphenol proteasome inhibitors: applications to rational drug design. *Proteins: Struct., Funct., Bioinf.* **2004**, *54*, 58–70.

(43) Chen, D.; Daniel, K. G.; Chen, M. S.; Kuhn, D. J.; Landis-Piwowar, K. R.; Dou, Q. P. Dietary flavonoids as proteasome inhibitors and apoptosis inducers in human leukemia cells. *Biochem. Pharmacol.* **2005**, *69*, 1421–1432.

(44) Mozzicafreddo, M.; Cuccioloni, M.; Cecarini, V.; Eleuteri, A. M.; Angeletti, M. Homology modeling and docking analysis of the interaction between polyphenols and mammalian 20S proteasomes. *J. Chem. Inf. Model.* **2009**, *49*, 401–409.

(45) Lei, M.; Zhao, X.; Wang, Z. L.; Zhu, Y. Q. Pharmacophore modeling, docking studies and synthesis of novel dipeptide proteasome inhibitors containing boron atoms. *J. Chem. Inf. Model.* **2009**, *49*, 2092–2100.

(46) Jones, G.; Willett, P.; Glen, R. C.; Leach, A. R.; Taylor, R. Development and validation of a genetic algorithm for flexible docking. *J. Mol. Biol.* **1997**, *267*, 727–748.

(47) *GOLD*, version 3.0; The Cambridge Crystallographic Data Centre: Cambridge, U.K., 2006.

(48) DeLano, W. L. *The PyMOL Molecular Graphics System*, version 0.99; DeLano Scientific: San Carlos, CA, 2006.

(49) Kimmel, C. B.; Ballard, W. W.; Kimmel, S. R.; Ullmann, B.; Schilling, T. F. Stages of embryonic development of the zebrafish. *Dev. Dyn.* **1995**, *203*, 253–310.

(50) *Insight II*; Accelrys Software Inc.: San Diego, CA, 2001.

(51) Zeng, J.; Liu, G. X.; Tang, Y.; Jiang, H. L. 3D-QSAR studies on fluoropyrrolidine amides as dipeptidyl peptidase IV inhibitors by CoMFA and CoMSIA. *J. Mol. Model.* **2007**, *13*, 993–1000.